

# A Novel Segmentation Algorithm for Range-Gated Images

Wang Guohua Wang Xinwei Zhang Yunfang Zhang Yiyun Zhou Yan Liu Yuliang

(*Optoelectronic System Laboratory, Institute of Semiconductors, Chinese Academy of Sciences, Beijing 100083, China*)

**Abstract** A novel algorithm to segment images under the echo broadening effect (EBE) in range-gated laser night vision technology is presented. The proposed algorithm uses average gray value of outline edges information to select the threshold extracting signal areas out. Spatial information of each pixel is applied to detect the noises from the candidate signal areas after the determination of the threshold. This algorithm avoids too much morphological operation and prevents the distortion of the images. The experimental results show that, using this method, it is very effective to segment low quality long distance range-gated images.

**Key words** imaging systems; range-gated image; image segmentation; echo-broadening effect; outline information, laser night vision

中图分类号 TP391 文献标识码 A doi: 10.3788/LOP49.091102

## 一种距离选通图像分割的新算法

王国华 王新伟 张运方 张逸韵 周燕 刘育梁

(中国科学院半导体研究所光电系统实验室, 北京 100083)

**摘要** 介绍了一种图像分割算法,用于受到距离选通激光夜视技术带来的回波展宽效应影响的图像。该算法利用有效信息区边缘线的平均灰度信息实现对分割图像阈值的选取以分割图像。选取该阈值后,算法利用空间信息实现对噪声的判断以除去噪声。该算法可以准确分割出有效信息区边缘,采用很少的形态学操作,保证了图像的还原质量。实验证明该算法可以准确地分割边缘模糊的距离选通激光夜视图像,对噪声等具有较强的稳健性。

**关键词** 成像系统;距离选通图像;图像分割;回波展宽效应;边缘信息;激光夜视

**OCIS codes** 110.1758; 100.3008; 100.3010

### 1 Introduction

Compared with passive imaging, laser-aided illuminating system has many advantages<sup>[1]</sup>. In recent years, active range-gated viewing technology based on the synchronization of a pulsed laser with a gating camera has attracted much attention in the applications of night remote surveillance, underwater imaging and three-dimensional (3D) imaging<sup>[1]</sup>. It overcomes atmospheric backscattering, providing high quality images even in bad weather conditions such as fog and snow. High quality imaging can be achieved in long distance (about 25 km), using laser illumination at 1.5  $\mu\text{m}$ <sup>[2]</sup>. Moreover, using depth scanning, distance (or depth, range) information of targets can be obtained, which has been extensively applied in three-dimensional imaging. Gate viewing is affected by the echo broadening effect (EBE)<sup>[3]</sup>. The intensity of signal areas can represent the distance between the location and the center location in signal areas. To obtain the accurate distance information, objects in range-gated images must be extracted out accurately. With this characteristic, the distance of every object in range-gated images can be measured in super-resolution. However, because of the EBEs the edges' intensity of signal areas grows gradually from noise areas. So the edges of signal areas are hardly discriminated from noise areas, which restricts the application of gate viewing. An algorithm is presented in this paper to extract signal areas out from images.

Many methods have been developed for binarization<sup>[4~10]</sup>. Methods based on the gradient, such as "Snake model"<sup>[10,11]</sup>, can segment objects from a plain background when there is an obviously gradient between them.

收稿日期: 2012-05-03; 收到修改稿日期: 2012-05-23; 网络出版日期: 2012-06-15

作者简介: 王国华(1987—),男,硕士研究生,主要从事图像处理方面的研究。E-mail: wangguohua@semi.ac.cn

导师简介: 刘育梁(1966—),男,研究员,博士生导师,主要从事光纤传感与智能光网络等方面的研究。

E-mail: ylliu@semi.ac.cn

However, these methods cannot segment such pictures' meaningless gradient information as the gray values change acutely on the same object. Histogram-based methods, such as Otsu's method<sup>[12]</sup> and the maximum entropy method<sup>[13]</sup>, can segment objects out of background when there is an obvious difference between gray values of objects and background. But histogram methods are only efficient when obvious object peaks exist in the histogram. In addition, these methods cannot keep details at objects' edges, which is very essential in our system as edges must be located accurately.

## 2 Introduction to range-gated images

In a range-gated image, noise areas are mainly constituted by black background where no laser can be backscattered when the camera gate is open. Noise pixels caused by the camera system and atmosphere turbulence are much less than black pixels, and noises contribute weakly to the final value when calculating the average gray value of the whole noise areas.

The signal-to-noise ratio (SNR) of night vision images is low<sup>[14]</sup>. The image quality of active imaging is mostly limited by atmospheric speckle noise<sup>[15]</sup>. Noises in noise regions always gather over four pixels with gray value just like edges while most of noise pixels are distributed on the low levels of a histogram. In the experiment the areas with low levels in histogram represent noise areas while nothing backscatters laser in the noise area. Due to the short time of range-gate, the low laser energy and the light attenuation during long distance, gray value of objects is low and changes dramatically. Edges of signal areas are discontinuous because of EBE. The energy back to camera is too low, and many pixels belonging to signals are totally dark or darker than the average gray value of noise areas. Under EBE, gray value of edge areas changes gradually from noise-like to signal-like areas. Analysis of a range-gated image is shown in Fig. 1. It is hard to discriminate edges from noise areas since noise near edge areas have same characteristics of edge pixels.

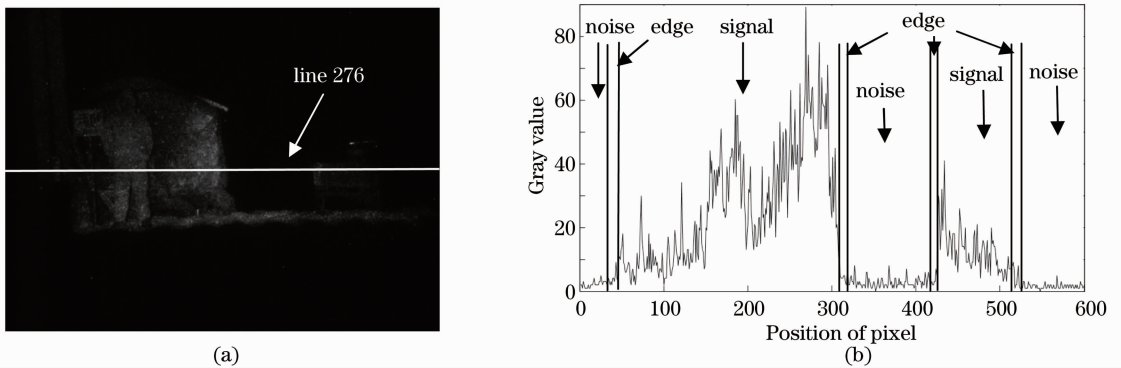


Fig. 1 Analysis of a range-gated image. (a) Source image; (b) gray values of pixels of line 276

The intensity of pixels in the 276th line is presented in Fig. 1. In signal areas, gray value changes dramatically and gray value of edge areas gradually changes to noise areas. Such edge characteristics in images are not considered in traditional adaptive partition algorithms, and the fuzzy edge cannot be located effectively. Using such algorithms, many pixels may be wrongly abandoned while the isolated pixel's gray value cannot be used directly. To solve the problems mentioned above, in the following parts, a new algorithm based on average gray value of signal areas' outline is proposed.

## 3 Algorithm based on outline information

### 3.1 Average gray value

A range-gated image can be illustrated by Fig. 2. Signal areas and noise areas are respectively the brightest and the darkest regions. Edge areas lie between signal and noise areas and edge areas are a part of the signal areas.

As shown in Fig. 2, the average gray value is obviously different among different areas. In the proposed algorithm, average gray values of the noise area (AVN) and edge area (AVE) are defined as

$$A_N = \frac{1}{n} \times \sum_{i \in N} v(i), \quad (1)$$

$$A_E = \frac{1}{n} \times \sum_{i \in E} v(i), \quad (2)$$

where  $A_N$  and  $A_E$  are respectively the average gray values of noise area and edge area;  $n$  is the number of pixels in noise area;  $v$  is the gray value of pixel being calculated.

### 3.2 Algorithm based on outline information

The novel method in this paper uses both the histogram information and edges' gray value changing information. By the change characteristics of edges' intensity, the average gray value of the candidate edge is bigger than that of noise areas. As the intensity changes slowly, AVE approximately equals AVN and a threshold should be set to distinguish the two different areas. In our experiment, the threshold is  $T_n(A_E - A_N) = 2$ .

An iteration process is created and shown in Fig. 3. Firstly, an initial threshold is determined, and images are segmented using this threshold. Then a morphological operation with a suitable structure element is taken to get the edges, and AVN and AVE are calculated. By calculating the difference between AVE and AVN, the algorithm can estimate whether the candidate edges are the needed areas. If the difference between them approximately equals 2, the result is acceptable and the iteration will end; if not, a new threshold can be got using the threshold minus 1.

Structuring element is the crucial part of mathematical morphology operations. Noise in images is usually different from signal areas. Noises always have around 4 pixel while the outside of edge areas are gathered denser. With this characteristic, morphology operation can eliminate noise and even edge pixels. An eight-connection region detection can discriminate most noise pixels.

To every edge pixel, a close operation can be introduced. The operation should use a suitable structure element, which can close edge pixels while keep signal areas outline well. Let  $S_e$  denote the structuring element which can be set as

$$S_e = \begin{bmatrix} 1 & 1 & 1 \\ 1 & 1 & 1 \\ 1 & 1 & 1 \end{bmatrix}. \quad (3)$$

The algorithm overcomes the impact of EBE, reduces the noise in the images and segments the object from the noise area effectively without many morphological operations. This keeps a certain image from distortion.

## 4 Experimental results and discussions

To show the advantages of the proposed algorithm, in the experiment, images are segmented using different algorithms and the results are compared. The images were captured by CCD camera and the experiments were finished on Matlab.

In the segmentation experiment, the image was captured in wild night. A tricycle and a tent were placed on the ground which was covered by the corn appearance like waves. Meanwhile, a man taking a plate stood in front of the tent. And two telecommunication poles were on the right of all other objects. The man was 300 m away from the camera, and the tent 329 m. The camera open time is 200 ns, and the SNR of the image is 42 dB. In our images, all the areas are viewed as signal areas. For the best algorithm, all the objects should be segmented out.

Results obtained from different algorithms are shown in Fig. 4. Obviously, the segmentation result is greatly improved using our algorithm. To better explain the differences with other algorithms, the threshold of the signal areas is exhibited. The threshold calculated by the maximum entropy algorithm is 54, which shows the worst picture

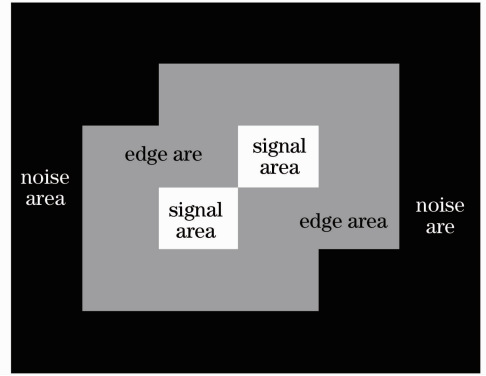


Fig. 2 Different areas in a range-gated image

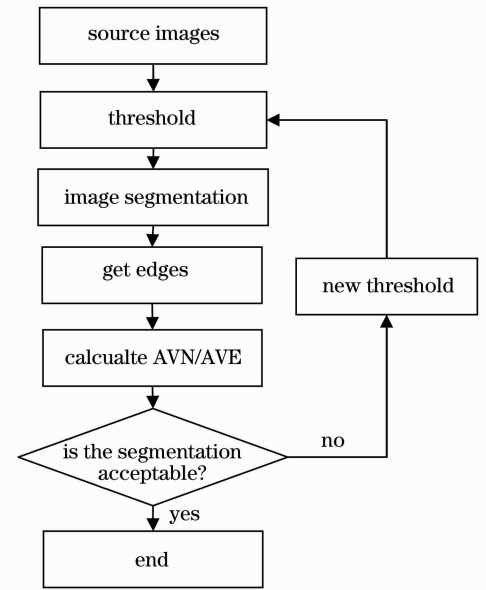


Fig. 3 Flow chart of outline based algorithm

throughout all the algorithms. Only signal areas with high gray values can be segmented out. Threshold calculated by the Otsu's algorithm is 26, the main figures of tent, people and the plate can be segmented out. However, the tricycle and telecommunication poles cannot be segmented out clearly. It is worth noting that the entire signal areas are segmented out effectively with the threshold calculated by the outline based algorithm being 4.

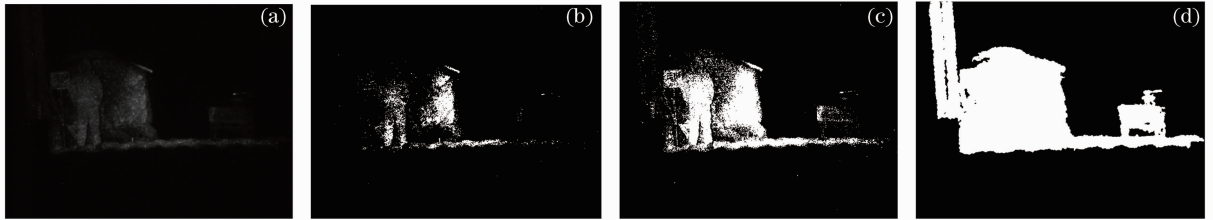


Fig. 4 Results obtained from different algorithms. (a) Source image; (b) maximum entropy algorithm; (c) Otsu's algorithm; (d) outline based algorithm

It is hard to calculate detection rate for all the signal areas when precise area cannot be got for most irregular shapes. We choose a region consisting of regular shape objects to calculate detection rate for different segmentation algorithms. The region and segmentation results are shown in Fig. 5.

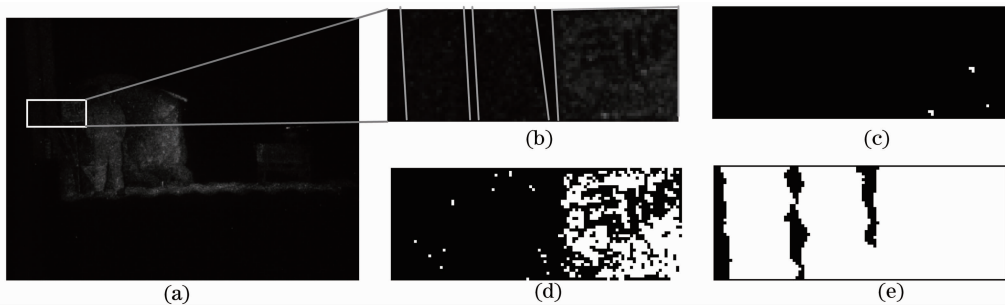


Fig. 5 Segmentation results of a region consisting of regular shape objects. (a) Source image; (b) selected region; (c) maximum entropy algorithm; (d) Otsu's algorithm; (e) outline based algorithm

As is shown in Fig. 5, objects in the region are marked in the source image. Only three little points can be detected by the maximum entropy algorithm, the detection rate is 0.2%, and the false alarm rate is 0; the plate is partly segmented out by the Otsu's algorithm, the detection rate is 25%; most signal areas can be segmented out by the outline based algorithm, the detection rate is 94%, and the false alarm rate is 7%. Segmentation using the proposed algorithm achieves a high quality. Compared with Otsu and maximum entropy algorithms, the outline based algorithm segments edge regions much better.

To show the segmentation effect on range-gated images under different scenes, segmentations on images of different scenes have been done. Edges in these images were set white while other areas were black; the width of edge was set 2 pixels in these experiments. In scene 1, a box was placed on the ground and a pole stood on the left; a box which was out of the range blocked the light in the middle of the image. These objects were about 150 m away from the camera. The camera open time is 80 ns, and the SNR of the image is 66 dB. The results of segmentation are shown in Fig. 6.

In scene 2, three plates were placed in our range, parts of them are blocked by smoke and cannot be seen. The distance between the plates and camera was 12 m. The camera open time is 40 ns, and the SNR of the image is 62 dB. The segmentation result is shown in Fig. 7.

Scene 3 is just the image segmented in Fig. 4. The segmentation result is shown in Fig. 8.

From Figs. 6~8, it is clearly seen that most signal areas in such images are segmented out accurately. In scene 1, the pole and box are segmented out, only the box distorts a little; in scene 2, all objects which can be detected by our eyes are segmented out accurately; in scene 3, all objects are segmented out, only poles and tricycle distort a little. It also shows that the algorithm is effective to eliminate noise pixels in those images while has nearly no obvious effect on the shape of signal areas.

The AVN, AVE and threshold results of these three scenes calculated in the process are shown in Table 1.

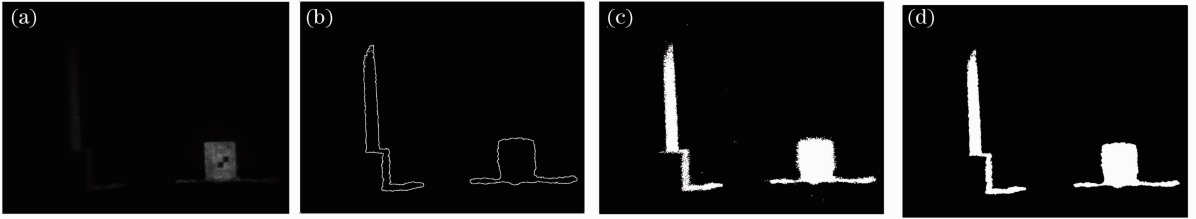


Fig. 6 Segmentation of scene 1. (a) Source image; (b) edge areas; (c) binarization result with noises; (d) segmentation result

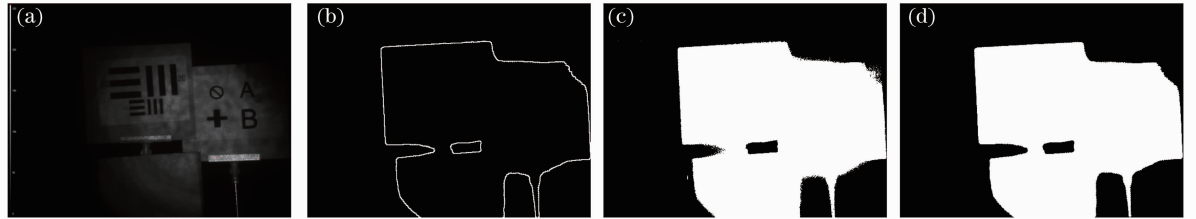


Fig. 7 Segmentation of scene 2. (a) Source image; (b) edge areas; (c) binarization result with noises; (d) segmentation result

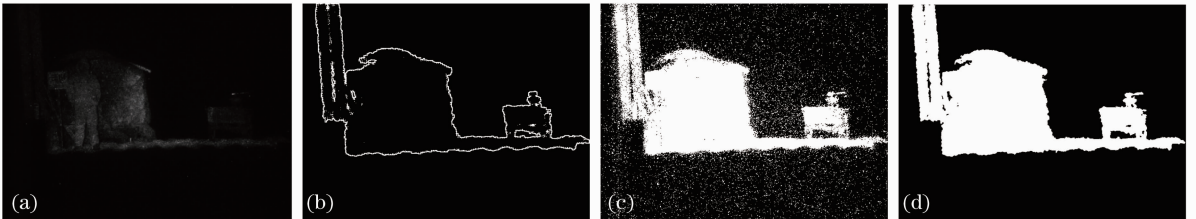


Fig. 8 Segmentation of scene 3. (a) Source image; (b) edge areas; (c) binarization result with noises; (d) segmentation result

Table 1 AVN, AVE and threshold of the three scenes

|                                | Scene 1 | Scene 2 | Scene 3 |
|--------------------------------|---------|---------|---------|
| AVN                            | 0.1971  | 0.8251  | 2.5261  |
| AVE                            | 2.1300  | 2.3304  | 4.1445  |
| Difference between AVE and AVN | 1.9329  | 1.5053  | 1.6184  |
| Threshold                      | 4       | 3       | 4       |

From Table 1, it is easy to see that while experiment environment is different, the AVN of each scene is quite different. The difference between AVE and AVN is different in different scenes. The outline based algorithm can adjust the difference of them and achieve accurate results.

## 5 Conclusion

A robust and non-parametric signal area segmentation algorithm is introduced. The proposed algorithm works well with range-gated laser night vision pictures under EBE. Gradually changing edges can be handled using this method. The proposed model is established based on the differences between average gray values of candidate signal areas' edges and those of noise areas. Threshold can be obtained precisely and is robust to the noises. Both the theory analysis and experimental results show that the algorithm could extract signal areas accurately. The segmentation results are acceptable for three-dimensional reconstruction of range-gated images.

## References

- 1 Liu Wei, Fu Jiangtao, Chang Benkang. Analysis on spectrum response and visual range of low light level night vision system under laser illumination [J]. *Chinese J. Lasers*, 2010, **37**(1): 312~315
- 2 刘伟, 付江涛, 常本康. 激光助视下微光夜视仪光谱响应和视距分析 [J]. *中国激光*, 2010, **37**(1): 312~315
- 3 Ove Steinvall, Pierre Andersson, Magnus Elmquist *et al.*. Overview of range-gated imaging at FOI [C]. *SPIE*, 2007, **6542**:

654216

- 3 Wang Xinwei, Zhou Yan, Fan Songtao *et al.*. Echo broadening effect in range-gated active imaging technique [C]. *SPIE*, 2009, **7382**: 738211
- 4 Sharon Alpert, Meirav Galun, Achi Brandt *et al.*. Image segmentation by probabilistic bottom-up aggregation and cue integration [J]. *IEEE Trans. Pattern Analysis and Machine Intelligence*, 2012, **34**(2): 315~327
- 5 Muhammad Kaleem, M. Sanaullah, M. Ayyaz Hussain *et al.*. Segmentation of brain tumor tissue using marker controlled watershed transform method [C]. *Communications in Computer and Information Science*, 2012, **281**: 222~227
- 6 Y. Bazi, L. Bruzzone, F. Melgani. Image thresholding based on the EM algorithm and the generalized Gaussian distribution [J]. *Pattern Recognition*, 2007, **40**(2): 619~634
- 7 Gamil Abdel-Azim, Z. A. Abo-Eleneen. Thresholding based on Fisher linear discriminant [J]. *J. Pattern Recognition Research*, 2011, **6**(2): 326~334
- 8 Shitong Wang, Fulai Chung, Fusong Xiong. A novel image thresholding method based on Parzen window estimate [J]. *Pattern Recognition*, 2008, **41**(1): 117~129
- 9 Indra Kanta Maitra, Sanjay Nag, Samir K. Bandyopadhyay. Detection of abnormal masses using divide and conquer algorithm in digital mammogram [J]. *International J. Emerging Sciences*, 2011, **1**(4): 767~786
- 10 Yue Wang, Zujun Hou, Xulei Yang *et al.*. Adaptive B-Snake model using shape and appearance information for object segmentation [J]. *International J. Numerical Methods in Biomedical Engineering*, 2011, **27**(5): 633~649
- 11 Michael Kass, Andrew Witkin, Demetri Terzopoulos. Snakes: active contour models [J]. *International J. Computer Vision*, 1988, **1**(4): 321~331
- 12 Nobuyuki Otsu. A threshold selection method from gray-level histograms [J]. *IEEE Trans. Systems, Man, and Cybernetics Society*, 1979, **9**(1): 62~66
- 13 Nikhil R. Pal, Sankar K. Pala. A review on image segmentation techniques [J]. *Pattern Recognition*, 1993, **26**(9): 1277~1294
- 14 Ma Shuang, Fang Jian'an, Sun Shaoyuan *et al.*. Colorizing algorithm of night-vision image based on clustering of false color fused image [J]. *Acta Optica Sinica*, 2009, **29**(6): 1502~1507  
马爽, 方建安, 孙韶媛等. 基于伪彩色融合图像聚类的夜视图像上色算法 [J]. *光学学报*, 2009, **29**(6): 1502~1507
- 15 Ove Steinvall, Pierre Andersson, Magnus Elmquist. Image quality for range-gated systems during different ranges atmospheric conditions [C]. *SPIE*, 2006, **6396**: 639607